

行政院國家科學委員會專題研究計畫成果報告

氮化鎵量子結構之設計及特性研究

論文報告: Optical Characterization of Mg-diffused GaN

計畫編號: NSC 89-2215-E-002-022

執行期限: 88年08月01日至89年07月31日

主持人: 詹國禎 台灣大學光電工程研究所

共同主持人: 林浩雄 台灣大學電機研究所

中文摘要

針對以 MOCVD 方式成長的氮化鎵晶體在 950°C, 不同擴散時間下達成鎂擴散的樣品, 進行光學特性量測, 經由二次離子質譜儀實驗, 在深度 2 μ m 內鎂濃度為 10¹⁸~10²⁰ atoms/cm³。光激發螢光光譜中所得之躍遷能譜, 分別對應中性施體及自由激子、深階施體至價電帶、施體受體間躍遷及其合併放出一個和兩個光聲子的能徵。

關鍵詞: 鎂擴散氮化鎵、光激發螢光光譜、拉曼頻譜

Abstract

Optical characterization for Mg-diffused GaN films grown by metal oxide vapor phase epitaxy is reported. The Mg-diffused GaN film specimens that were prepared and diffused with varied time at temperature 950°C in the furnace. The Mg concentration of 2 μ m GaN layer is within the range 10¹⁸~10²⁰ atoms/cm³ measured by secondary ion mass spectroscopy. Optical transition energy features displayed on PL spectrum are characterized and identified. The neutral donor bound exciton and free exciton A, deep donor to valance band, donor-to-acceptor pair and replica with one and two longitudinal phonons optical transitions were observed.

Keywords: Mg-diffused GaN, optical characterization, photoluminescence, Raman scattering spectroscopy.

I. INTRODUCTION

Recently, much attention was paid on GaN-based semiconductors for their potential in opto-electronic and electronic device applications [1,2]. Highly efficient GaN-based green and blue light

emitting diodes have been fabricated, and a successful realization of the blue laser diode has been reported recently [3]. However, one of the key requirements for high performance devices is to grow high quality GaN layers and p-type GaN. Unfortunately, the as-grown Mg-doped GaN films grown by metal organic chemical vapor deposition (MOCVD) are semi-insulating because of the low activation efficiency of Mg.

In this paper we report the optical characterization on Mg-diffused GaN layers by several measurement techniques. The experimental results that provide useful information about the electronic structure of Mg-diffused impurities in GaN film.

II. EXPERIMENTS

Wurtzite structure GaN film on sapphire substrate was grown by MOVPE system. The substrate orientation leads to films with a wurtzite c axis perpendicular to the surface. Mg-diffusion GaN film was formed by Mg diffusion into MOVPE grown undoped n-type GaN to achieve p-type GaN using Mg₃N₂ as the Mg source. The MOVPE grown GaN on sapphire with about 2 μ m undoped layer with a carrier concentration $\sim 5 \times 10^{16}$ cm⁻³ was sealed with Mg₃N₂ powder in a vacuum quartz ampoule. Then the ampoule with the GaN samples S₁, S₂, S₃ and S₄ were put in a 950°C furnace for 15 min, 1 hr, 4 hrs and 16 hrs diffusion process, respectively.

Raman scattering measurements were performed in the backscattering configuration with the same accumulation time by a Dilor XY800 triple-grating Raman Spectroscopy equipped with a microscope. All spectra were excited by the

514.5 nm line of an Ar⁺ laser and recorded by a liquid N₂ cooled CCD. The laser power was kept below 5 mW to avoid local heating effect. For the Raman spectra, the line shape for the optical phonons are assumed to be Lorentzian.

Photoreflectance measurements were carried out at room temperature, using a 20 mW He-Cd 325 nm laser as pumping light and a 150W Xe-arc lamp as the probe light. Photoreflectance spectra were fitted by the third derivative Gaussian functional form to obtain the transition energy and other parameters such as the amplitude and the broadening parameter.

III. RESULTS AND DISCUSSION

The results of Mg profile measurements using secondary ion mass spectroscopy (SIMS) technique are displayed in Fig. 1. The Mg concentration (atoms/cc) over entire GaN layer were at the range of 10^{18} ~ 10^{20} atoms/cm³. The integrated values of SIMS profile measurements within the 2 μ m GaN were 1.58×10^{20} , 1.66×10^{20} , 3.29×10^{20} , and 2.43×10^{21} (in atoms/cm²). The Mg concentration increases as diffusion time increases.

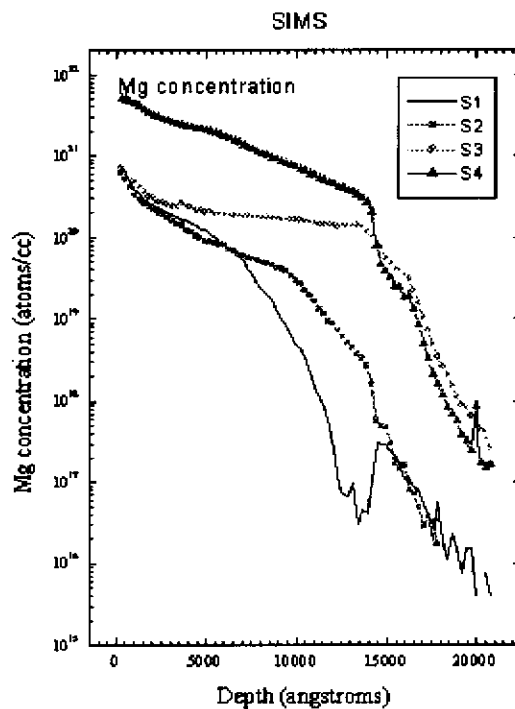


Fig. 1 SIMS profile for the GaN samples processed at 950°C for 0.25(S₁), 1hr.(S₂), 4hrs.(S₃), and 16hrs.(S₄).

PL spectra for varied diffusion time at temperature 50 K are displayed in Fig.2. The spectra have been normalized with respect to the E₁ transition amplitudes and offset-shifted by half-decade order for viewing. The energy values of the optical transitions E₁, E₂, E₃, E₄ and E₅ are also fitted by a Lorentzian function from PL spectra for varied diffusion time and the experimental results are summarized in Table I.

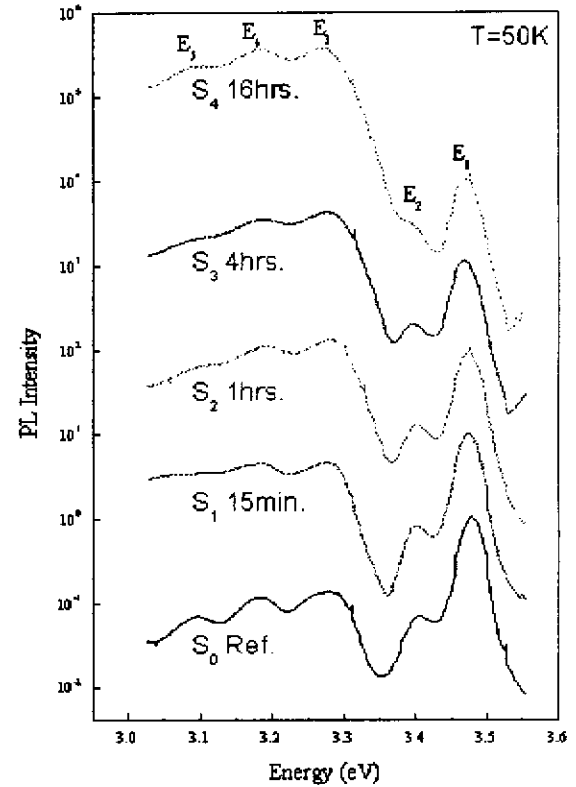


Fig. 2 Photoluminescence spectra of samples at 50 K.

TABLE I SUMMARY RESULTS OF OPTICAL MEASUREMENTS OF ALL THE SAMPLES.

		S ₀	S ₁	S ₂	S ₃	S ₄
Photoluminescence	E ₁	3.478	3.474	3.474	3.469	3.469
	E ₂	3.412	3.412	3.400	3.400	3.400
	E ₃	3.274	3.277	3.282	3.279	3.270
	E ₄	3.185	3.191	3.277	3.412	3.478
	E ₅	3.095	3.069	3.124	3.106	3.108
Photoreflectance	Energy (eV)	3.421	3.409	3.413	----	3.416
	Broaden (meV)	12.1	19.1	15.0	----	14.3
Raman Scattering Spectroscopy	Wave Number	736.0	736.9	737.4	----	736.3
Hall Measurement	Type	n	n	p	----	p
	Concen. 10 ¹⁶ cm ⁻³	-1.29	-0.235	25.0	----	5.25

The energy differences between peak E_1 and peak E_2 from PL results are around 62~69 meV. The peak E_2 is responded from deep donors to valance band transition. The binding energy of ΔE_{DD} state has been estimated as E_{DD} around (100 ± 3) meV in Ref.[4]. Such deep donors can be intrinsic defects. It is used to interpret the E_2 energy feature in the PL spectrum of sample S_0 .

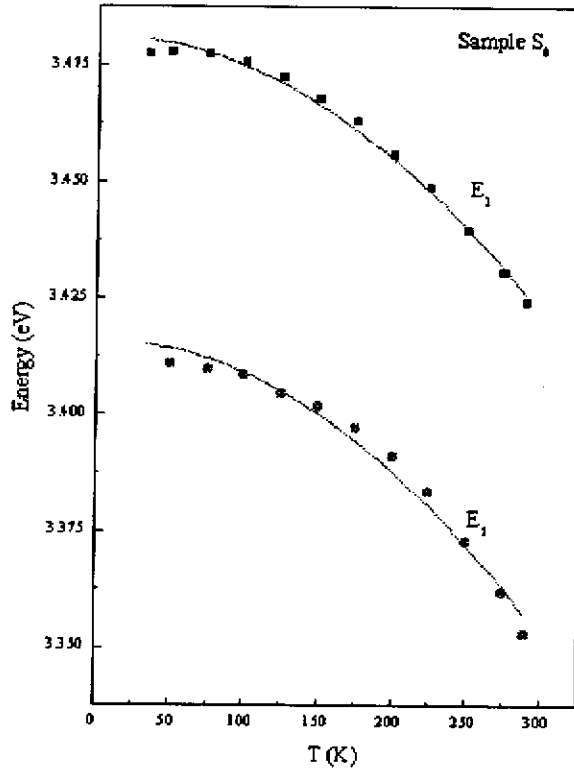


Fig. 3 The temperature dependence of the optical transitions E_1 and E_2 for sample S_0 . The solid curve is calculated by Varshni's equation using published results [5].

Fig. 3 shows the temperature dependence of E_1 and E_2 optical transitions measured from PL spectra for the reference sample S_0 . The solid curve is calculated by Varshni's equation using published data [5]. The parameters of $E_g(0)$, α and β are 3.489 eV, $8.87 \cdot 10^{-4}$ eV/K² and 874 K, respectively. The experiment data is good agreement with the calculated values above the temperature 150K. However, below 150 K, the curve does not fit well. These suggest the E_1 transition may be attributed to the FXA and D^0X transitions. The D^0X optical transition is quenched above temperature 150 K. Because the activation

energy of D^0X is 14 meV measured from intensity integration of PL spectrum. Therefore, the temperature increases and the D^0X is thermalized and the FXA transition peak is dominant.

The energy level Mg acceptor above the valance band is 200 meV. The energy difference between E_1 and E_3 peak is about 204 meV. The E_3 is responded form the DAP optical transition which are contributed by the Mg-diffusion.

Raman scattering spectra at room temperature are shown in Fig. 4. The GaN LO phonon frequencies of all samples are about 736 cm^{-1} . And the consecutive separations between E_3 , E_4 , and E_5 in PL spectra are 89 meV and 90 meV, respectively. These values are consistent with the energy of GaN LO phonon. Thus, we identified peak E_3 as the donor-to-acceptor pair (DAP) transition. The peaks E_4 and E_5 are one DAP with one longitudinal phonon (1 LO) and two longitudinal phonons (2 LO) replica transitions, respectively.

Fig. 5 display the PR spectra for sample S_0 , S_1 , S_2 , S_4 over the range of 3.2 to 3.5 eV. The solid lines are fitting curves by third derivative Gaussian function form. And the fitting parameters are listed in Table I. The PR signals on the low-energy side of the main peak may be attributed to the interference caused by multiple layer reflection.

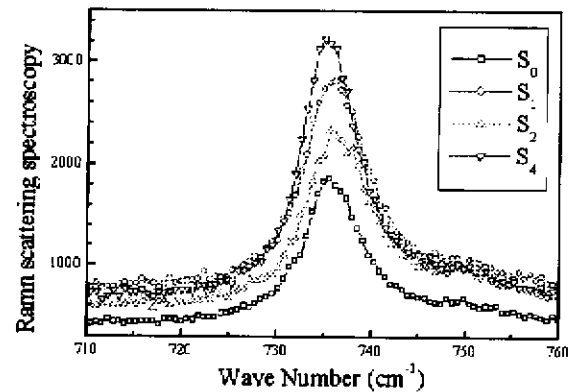


Fig. 4 Room temperature Raman spectra of samples S_0 , S_1 , S_2 , S_4 .

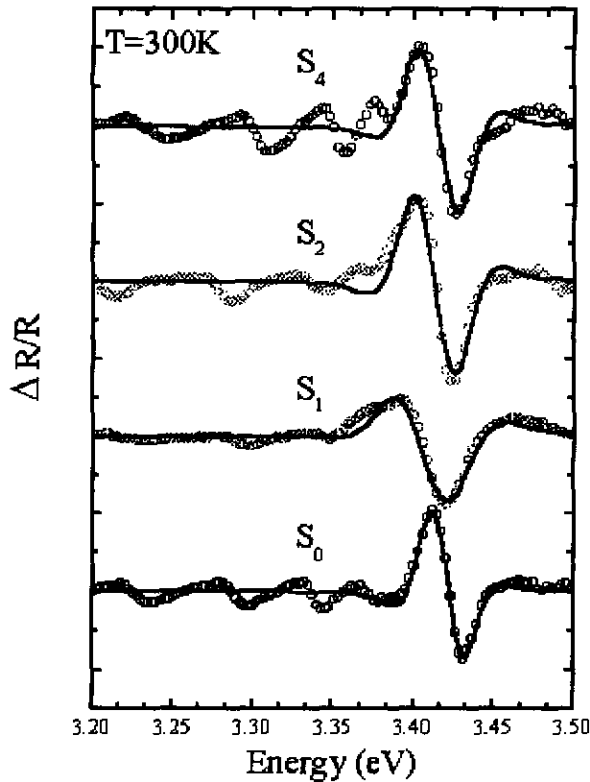


Fig. 5 Photoreflectance spectra of samples at room temperature. The solid lines are fitting curves.

As shown in the Table I, the bandgap transition energies of samples are slightly different, due to the doping effect. The bandgap renormalization effect has to be treated by the many-body theory, and for bulk materials, the band-gap shrinkage is given by Ref.[6]

$$\Delta E_g = E_g - E_0 = -K(n^{1/3} + p^{1/3})$$

where n and p are the n-type and p-type carrier concentration, respectively. E_0 is the intrinsic energy band gap, whereas E_g is the energy-band gap in the presence of excess carriers. The proportional constant K is $(2.4 \pm 0.5) \times 10^{-8}$ eVcm [7]. The results of the room-temperature Hall measurement show that the carrier concentrations for sample S_0 , S_1 , S_2 , S_4 are 1.29×10^{16} , 2.35×10^{15} , 2.5×10^{17} , and 5.25×10^{16} cm⁻³, respectively. The shrinkage energy difference between S_1 , S_2 , S_4 and S_0 are -2.4, 9.5, and 3.4 meV, respectively. These values are comparable with the PR results, except sample S_1 . Since the

Mg diffusion profile along the depth was not uniform, the measured results only reflected an average value over the entire GaN layer with about 2 μ m. In Fig. 1, the Mg profile of sample S_1 rapidly decay at the depth 0.6 μ m. So, the carrier concentration measured by Hall effect is very different the concentration near surface.

IV. SUMMARY

Several measurement techniques have been employed to study the optical properties of electron transition in Mg-diffused P-type GaN epilayer grown by MOPVE. The defect-related deep donor to valance band optical transition has been observed and identified. The free exciton, donor to acceptor, DAP-1LO and DAP-2LO transitions were also characterized. The PL spectroscopy could offer a diagnostic tool to investigate the defects such as intrinsic or extrinsic defect (Mg diffusion enhanced defect). It also provides an optical characterization to measure Mg concentration of ionized acceptor from DAP energy features.

From the PR spectra, the bandgap renormalization are observed and confirmed by room temperature Hall measurement.

REFERENCE

- [1] S. Nakamura, S. Masayuki, S. Nagahama, N. Iwasa, T. Yamada, T. Mat-sushita, Y. Sugimoto, and K. Hiroyuki, *Appl. Phys. Lett.*, Vol. 70, pp. 1417-1419, 1997.
- [2] S. Chichibu, T. Azuhata, T. Sota, and S. Nakamura, *J. Appl. Phys.*, Vol. 79, pp. 2784-2786, 1996.
- [3] S. Tanaka, S. Iwai, and Y. Aoyagi, *Appl. Phys. Lett.*, Vol. 69, pp. 4096-4098, 1996.
- [4] V. Yu. Nekrasov, L. V. Belyakov, O. M. Sreseli, and N. N. Zinov'ev, *Semiconductos*, Vol. 33, pp. 1284-1290, 1999.
- [5] M. Leroux, N. Grandjean, B. Beaumont, G. Nataf, F. Semomd., J. Massies, and P. Gibart, *J. Appl. Phys.* Vol. 86, pp. 3721-3728, 1999.
- [6] H. C. Casey and F. Stern, *J. Appl. Phys.*, Vol. 47, pp. 631-643, 1976.
- [7] X. Zhang, S. J. Chua, W. Liu, and K. B. Chong, *J. of Crystal Growth*, Vol.189, pp. 687-691, 1998.